Lab on a Chip

Cite this: *Lab Chip*, 2012, **12**, 3694–3699

www.rsc.org/loc

PAPER

Atmospheric-pressure microplasma in dielectrophoresis-driven bubbles for optical emission spectroscopy†‡

Shih-Kang Fan,*[a] Yan-Ting Shen,[b] Ling-Pin Tsai,[b] Cheng-Che Hsu,[c] Fu-Hsiang Ko[b] and Yu-Ting Cheng[d]

Received 2nd May 2012, Accepted 23rd July 2012
DOI: 10.1039/c2lc40499k

The manipulation of bubbles and the ignition of microplasma within a 200 nL bubble at atmospheric pressure and in an inert silicone oil environment were achieved. Driven by dielectrophoresis (DEP), bubble generation, transportation, mixing, splitting, and expelling were demonstrated. This process facilitated the preparation of various bubbles with tuneable gas compositions. Different gas bubbles, including air, argon (Ar), helium (He), and Ar/He mixtures, were manipulated and ignited to the plasma state by dielectric barrier discharge (DBD) within a 50 μm-high gap between parallel plates. Moving and splitting the atmospheric-pressure microplasma in different gas bubbles were achieved by DEP. The excited light of the microplasma was recorded by an optical spectrometer for the optical emission spectroscopy (OES) analyses. The characteristic peaks of air, Ar, and He were observed in the DEP-driven microplasma. With the capability to manipulate bubbles and microplasma, this platform could be used for gas analyses in the future.

Introduction

The history of chemical spectrum analyses dates back to the mid-19th century, when Kirchhoff and Bunsen observed the characteristic emission spectrum.[1] Individual elements were introduced into a flame and analysed by atomic emission spectroscopy of the emitted radiation. The spectral intensity of a particular element was found to change with the amount of the element for both the qualitative and quantitative analyses. Similar to a flame, plasma provides sufficient energy to cause excitation, dissociation, and ionisation of atoms and molecules.[2] In plasma, the electron transition between energy states leads to characteristic spectrum emission. The emission spectra that are obtained are therefore used to analyse the composition of the analyte through different characteristic peaks, making plasma an efficient tool for analytical purposes. For example, helium, methane, nitrogen, and air gases have been analysed using the emission spectra from plasma.[3,4]

In addition to gas analyses, plasma has also been widely used in various industrial applications. Recently, micoplasma[5,6] and atmospheric-pressure plasma[7,8] have drawn considerable attention due to their wide applications, including those related to the biomedical field. However, a large amount of carrier gas consumption is necessary for most plasma systems. A plasma system with high efficiency and low sampling gas and carrier gas consumption is urgently required, especially for analytical purposes such as inductively coupled plasma optical emission spectroscopy (ICP-OES). Demonstrated on microfluidic devices, plasma has been generated along microchannels with continuously flowed gas for applications such as gas chromatography,[9] surface modification,[10] and others.[11,12]

Here, we report a novel approach to realise microplasma in a bubble having a specific gas volume and composition without carrier gas flowing on a chip. Spatial and temporal manipulations of individual and discrete droplets and bubbles have been intensively studied in the field of digital microfluidics (DMF).[13,14] As droplets provide a convenient way to handle various liquids with specific volumes, bubbles facilitate quantitative gas sample preparations. Bubble manipulations have been demonstrated in water and oil by electrowetting-on-dielectric (EWOD)[15] and dielectrophoresis (DEP),[16] respectively. Driving bubbles in oil by DEP is used here because water cannot sustain the strong electric field for plasma ignition. With the ability to manipulate bubbles by DEP, unknown gas samples and reference gas bubbles can be generated, transported, mixed, split, and expelled on the platform before being excited to a plasma state at room temperature and atmospheric pressure. They can then be analysed by optical emission spectroscopy (OES).

Principle

Dielectrophoresis

DEP draws fluids of higher permittivity into a strong electric field region of lower permittivity.[17–21] With the DEP actuations,

[a]*Department of Mechanical Engineering, National Taiwan University, Taipei, 10617, Taiwan E-mail: skfan@fan-tasy.org*
[b]*Department of Materials Science and Engineering, National Chiao Tung University, Hsinchu, Taiwan*
[c]*Department of Chemical Engineering, National Taiwan University, Taipei, Taiwan*
[d]*Department of Electronics Engineering, National Chiao Tung University, Hsinchu, Taiwan*

† Published as part of a themed issue on optofluidics

‡ Electronic supplementary information (ESI) available: Ar and He bubble generation, mixing, splitting, and expelling (Video 1); microplasma moving (Video 2); microplasma moving in dark (Video 3); microplasma splitting (Video 4); microplasma breaking (Fig. S1); microplasma moving in dark (Fig. S2)

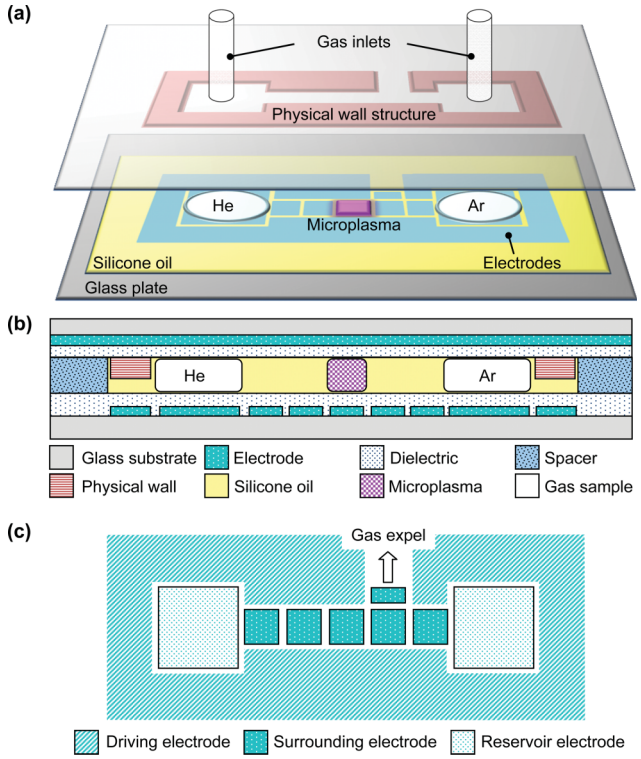

Fig. 1 Design of the parallel plate device for bubble and microplasma manipulations in silicone oil. (a) Angled view of the device with two gas inlets, reservoirs, physical wall structures, and patterned electrodes for bubble and microplasma studies. (b) Cross section of the device. (c) Top view of electrode design on the bottom plate.

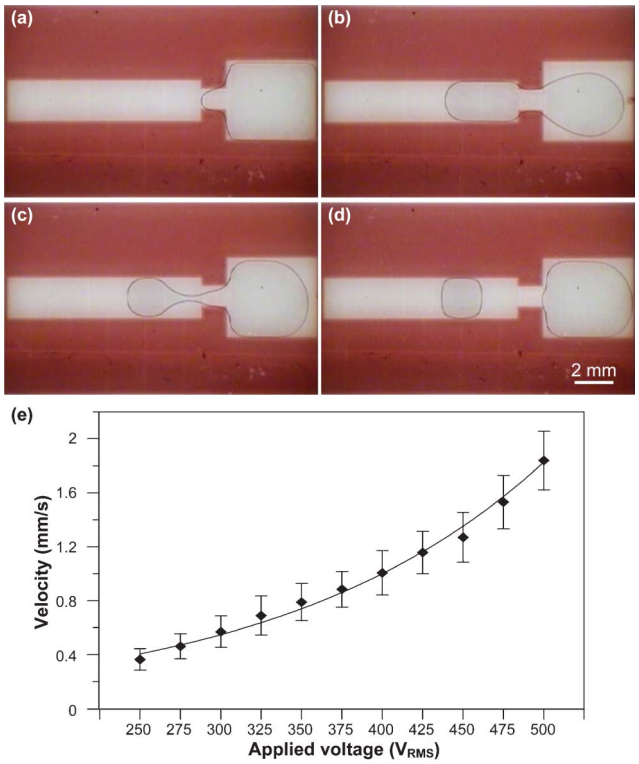

Fig. 2 Air bubble (200 nL) manipulations by DEP. (a)–(d) Generating an air bubble from the gas reservoir by applying 250 V_{RMS}, 2.4 kHz. (e) The velocity of the generated bubble plotted against the applied voltage at 2.4 kHz. Each data point was averaged from experiments on 3 devices, and each device performed 4 experiments.

we have successfully pumped water continuously along a virtual microchannel in an oil environment[22] and discrete oil droplets in air.[23,24] Here, we inversely drive gas bubbles with lower permittivity in a surrounding medium, such as silicone oil, with higher permittivity by DEP.[16] The normal stress (force density) or pressure difference caused by DEP at the medium-gas interface acting from the medium to the gas is:[19]

$$\Delta P_{DEP} = \frac{\varepsilon_0(\varepsilon_M - \varepsilon_G)}{2} E^2 \quad (1)$$

where E is the electric field intensity, ε_0 (8.85×10^{-12} F m^{-1}) is the permittivity of vacuum, and ε_M and ε_G are the relative permittivity of the medium and the gas, respectively. In our experiment, gas ($\varepsilon_G \approx 1$) bubbles were expelled from a strong electric field by DEP in 20 cSt silicone oil ($\varepsilon_M = 2.5$).

Microplasma ignition

Dielectric barrier discharge (DBD)[2,25] was adopted for observation and detection purposes because stable and low temperature plasma can be obtained. These features are beneficial to device operation and the acquisition of an optical signal. The major parameters affecting the plasma ignition include the gas species, gas pressure, applied voltage, and the distance between electrodes. Different types of gas under the same environmental conditions have different breakdown voltages. Gas pressure mainly affects the mean free path of gas atoms or molecules, which in turn influences the energy they gain between collisions.

The applied voltage and spacer height are the energy factors that influence the gas breakdown. According to Paschen's law,[2] the product of gas pressure (P) and electrode spacing (d) determines the breakdown voltage (V_b) as described by:

$$V_b = \frac{B(P{\cdot}d)}{\ln[A(P{\cdot}d)] - \ln\left[\ln\left(1 + \frac{1}{\gamma_{se}}\right)\right]} \quad (2)$$

where A and B are the parameters from experiments and γ_{se} is the cathode secondary electron emission coefficient. In our experiments, microplasma was ignited in the bubbles at atmospheric pressure. From the Paschen curves of argon (Ar) and helium (He) in the literature,[2] we decided to space the electrodes on the parallel plates 50 μm apart to minimise the required breakdown voltage. Ar and He bubbles were employed because noble gases render simpler energy level transitions and clearer characteristic optical emission peaks for the spectroscopic analysis. A voltage of 400 to 800 V_{RMS}, 2.4 kHz was applied to ignite the gas bubble to the plasma state.

Experimental setup

A bubble manipulation device for gas analysis by OES was designed with two glass plates as shown in Fig. 1. The indium tin oxide (ITO, 200 nm-thick) coated on the bottom glass plate (0.7 mm-thick) was patterned by photolithography and wet etching processes. As shown in Fig. 1(c), three different electrodes

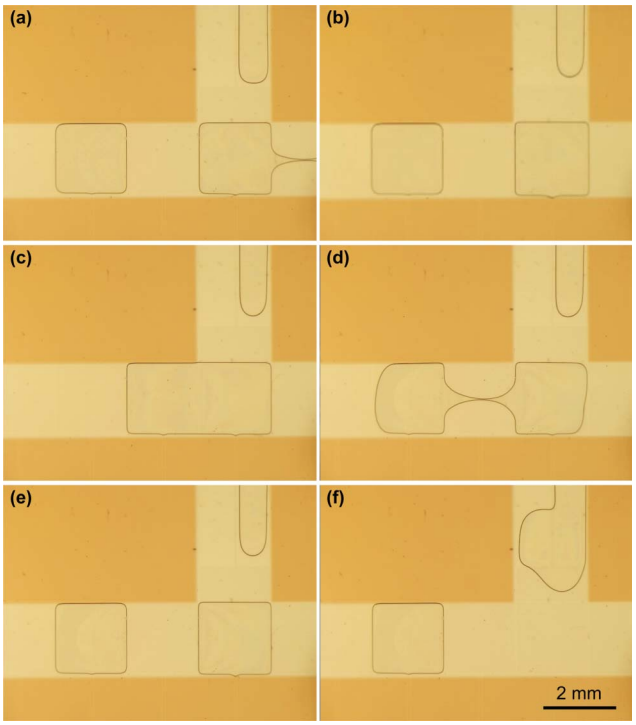

Fig. 3 Manipulations of bubbles. (a)–(b) Creating Ar (left) and He (right) bubbles. (c) Merging and mixing Ar and He bubbles. (d)–(e) Splitting the Ar/He mixture bubble. (f) Expelling one of the split Ar/He mixture bubbles. The voltage applied here was 315 V_{RMS} at 2.4 kHz. See supplementary Video 1, ESI.‡

were designed. Driving electrodes (2 mm × 2 mm) were used for bubble manipulations and microplasma ignition. Surrounding electrodes prevented the bubbles from moving away from the driving electrodes. Reservoir electrodes positioned the large bubble of the gas reservoir. Negative photoresist SU-8 (SU-8 2002, MicroChem) was spun on the bottom plates containing patterned electrodes as a 1.8 μm-thick dielectric layer for DBD. The top glass plate contained an unpatterned ITO electrode and a SU-8 layer. A layer of 10 μm-thick AZ P4620 (Clariant) positive photoresist was applied and patterned as a physical wall structure on the top plate with the same shape as the bottom surrounding electrode to confine the bubbles on the appropriate electrodes. In some experiments, two holes on the top plate were machined for fixing two glass tubes (3 mm outer diameter and 2 mm inner diameter) as the gas inlets, as shown in Fig. 1(a). The top and bottom plates were assembled using 50 μm-high double-sided tape spacers. Silicone oil (20 cSt, Dow Corning Corp.) and gas were

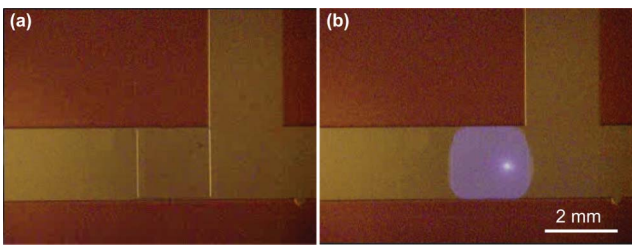

Fig. 4 Ar microplasma ignition from a gas state (a) to a plasma state (b) by applying 693 V_{RMS}, 2.4 kHz.

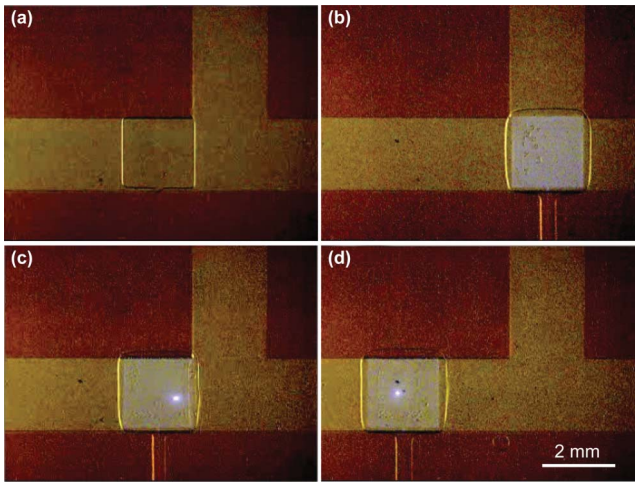

Fig. 5 Ar microplasma ignition and transportation with 655 V_{RMS}, 2.4 kHz applied. See also Video 2, ESI‡.

carefully introduced in the device. The assembled devices (Fig. 1(b)) were placed above an optical spectrometer (USB4000, Ocean Optics) for OES recordings and under a stereo microscope (SZX16, Olympus) for bubble and microplasma observations. A function generator (33210A, Agilent Technologies) was connected with an amplifier (623B, Trek) to supply the bubble driving voltage and microplasma igniting voltage. The bubbles were driven through relays (LU-5, Rayex Electronics) switched by the digital output signals of a data acquisition device (USB-6251, National Instruments) programmed using the LabVIEW software.

Results and discussion

Bubble generation and transportation

Fig. 2 shows the schematic for bubble generation on a device with only one gas reservoir filled with air. Air was first pushed onto the driving electrodes while applying 250 V_{RMS}, 2.4 kHz on

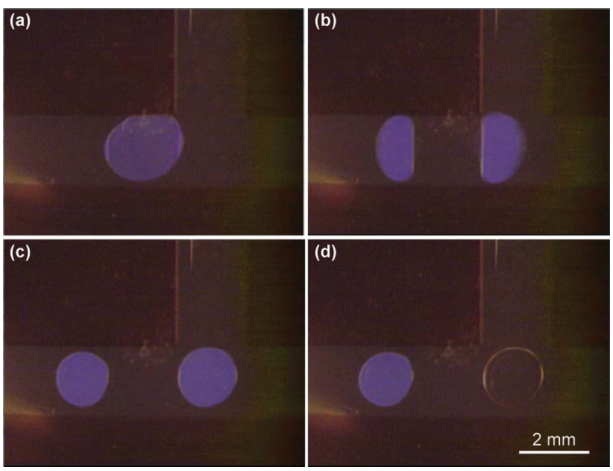

Fig. 6 Microplasma splitting. (a)–(c) A single microplasma bubble was split into two microplasma bubbles with a 587 V_{RMS}, 2.4 kHz signal. (d) The microplasma on the right was extinguished by turning of the electric field. See also Video 4, ESI‡.

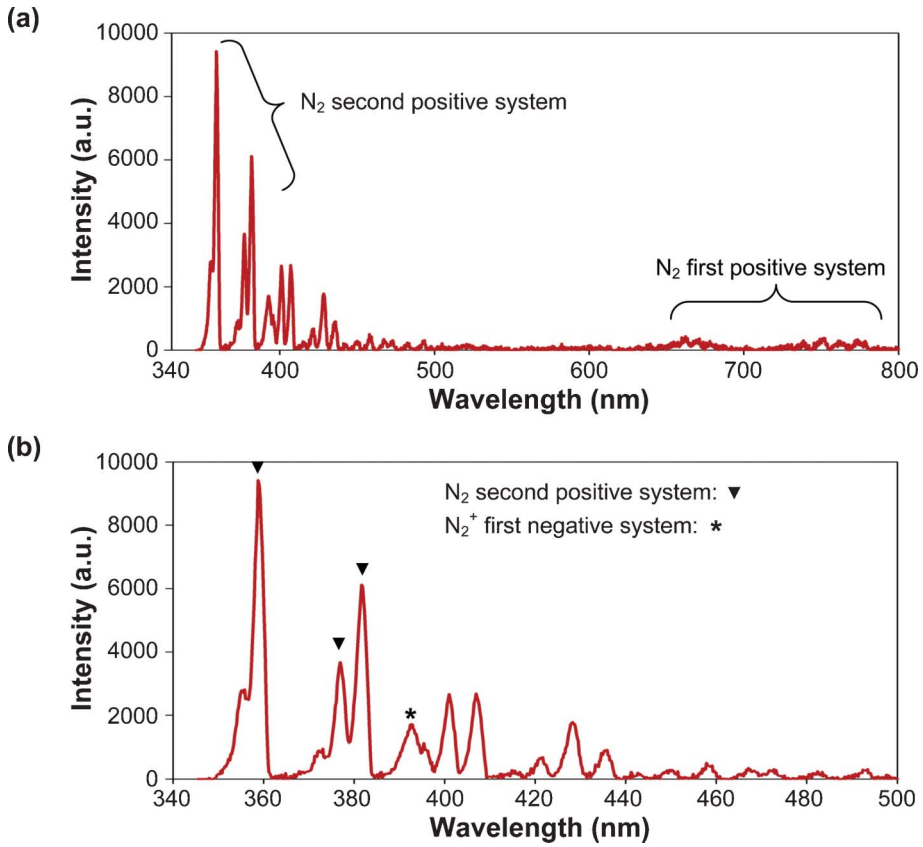

Fig. 7 The optical emission spectrum of the air microplasma with 703 V_{RMS}, 2.0 kHz applied. (a) Spectrum shown between 340 and 800 nm. (b) Magnified spectrum shown between 340 and 500 nm.

the reservoir electrode to attract silicone oil by DEP as shown in Fig. 2(a) and 2(b). A 200 nL air bubble was generated by turning on the electrodes between the bubble and the reservoir to attract silicone oil and cut the air sample off as shown in Fig. 2(c) and 2(d). Based on previous studies,[23,24] electric signals with other frequencies (*e.g.*, DC) can also be used to generate DEP forces and drive bubbles. A frequency of 2.4 kHz is used mainly because it is beneficial for microplasma ignition. With this scheme, 200 nL air, He, and Ar bubbles were successfully generated and then transported by DEP.

The bubble transportation velocities of air, Ar, and He were measured by fixing the applied voltage and adjusting the electrode switching time. At a certain applied voltage, the electrode switching time was decreased until the bubble did not follow the control signals. The maximum velocity of the bubbles at various applied voltages was recorded and plotted in Fig. 2(e). Each data point represents an averaged voltage from 12 experiments using 3 different devices The best-fit quadratic curves indicate that the velocity is proportional to the square of the applied voltage, or the DEP force of eqn (1). Because the permittivity of air, Ar, and He is close to 1, no differences were found between different gas bubbles that were tested. In this experiment, the maximum velocity of bubbles was 1.84 mm s^{-1} at 500 V_{RMS}. Higher voltage could be applied to achieve a higher velocity. With voltages above 500 V_{RMS} (*i.e.*, the electric field strength above 10 MV m^{-1}), however, gas breakdown was found in bubbles to generate plasma.

Bubble mixing, splitting, and expelling

Two different gas bubbles were generated, transported, mixed, and split on the device with two gas reservoirs as shown in Fig. 1. Fig. 3 shows the centre driving electrode part of the device. As shown in Fig. 3(a) and 3(b), an Ar bubble was generated from the Ar reservoir on the right (not shown), and a He bubble was generated from the He reservoir on the left (not shown) using the scheme shown in Fig. 2. Because DEP was applied to attract silicone oil and push away the bubble, the surrounding electrode was always turned on to keep the bubble on the driving electrodes. The physical wall structure also helped to hold the bubbles. The two bubbles were merged to form an Ar/He mixture bubble (Fig. 3(c)). The mixed bubble was split into two bubbles with the same composition as shown in Fig. 3(d) and 3(e). The bubble on the right was expelled (Fig. 3(f)), while the bubble on the left could be investigated in the steps that followed, including microplasma ignition. Precise mixing and splitting of the bubbles would sequentially dilute one of the gas bubbles for quantitative detection. For example, an unknown gas sample can be diluted with a reference gas (*e.g.*, Ar or He) at a desirable ratio for microplasma ignition and OES spectroscopy.

Microplasma ignition and manipulations

Fig. 4 shows an image of microplasma ignition in an Ar bubble when applying a 693 V_{RMS}, 2.4 kHz electric signal. As described

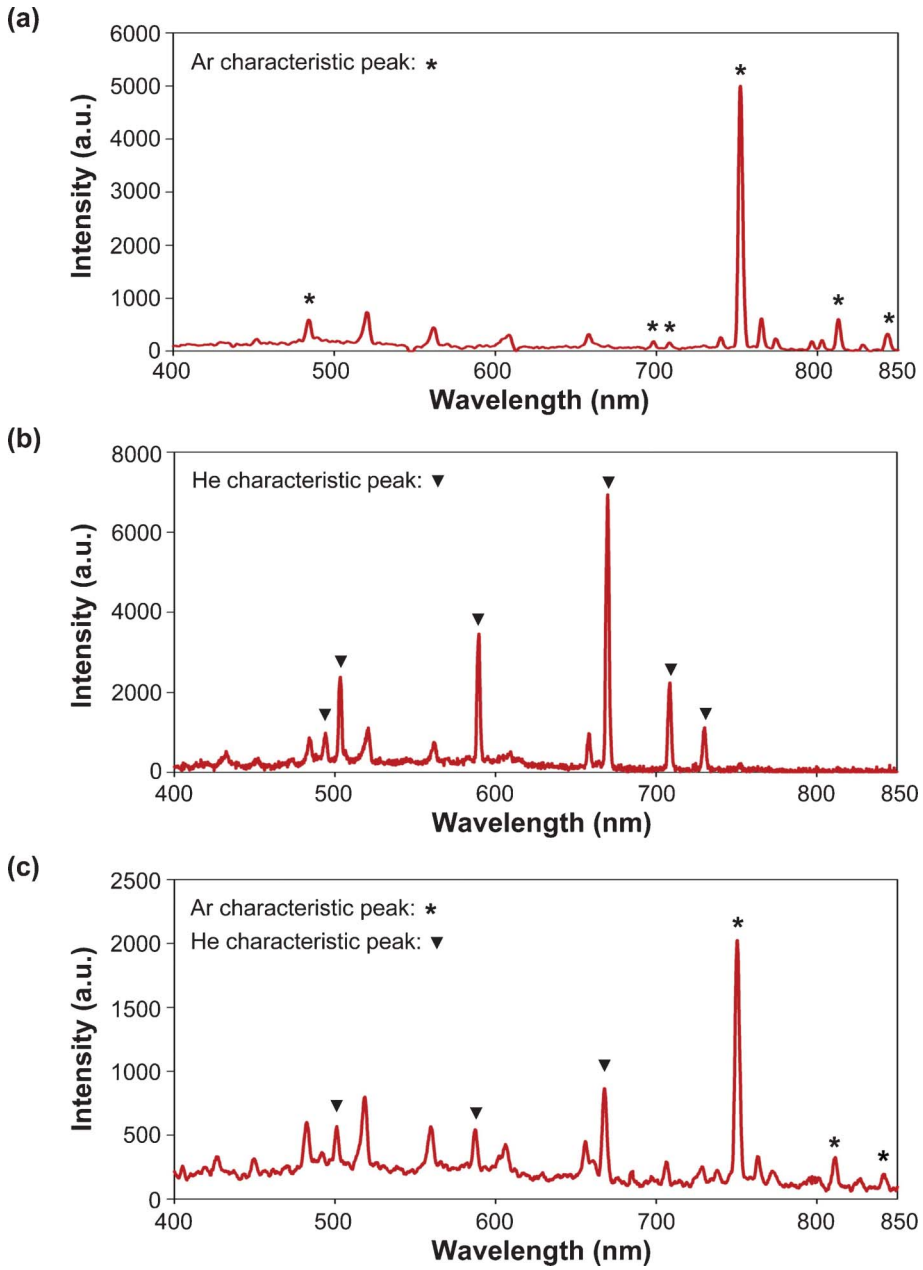

Fig. 8 The optical emission spectra of the microplasma for different bubbles. (a) Ar spectrum (482 V_{RMS}, 2.4 kHz) with characteristic peaks highlighted by an asterisk (*). (b) He spectrum (502 V_{RMS}, 2.4 kHz) with characteristic peaks highlighted by the following symbol: ▼. (c) Ar/He mixture spectrum (523 V_{RMS}, 2.4 kHz) with both characteristic peaks highlighted.

above, the bubbles were pushed away from the high electric field region by DEP and positioned at the low electric field region with no voltage applied. However, to ignite the microplasma in the bubble, a sufficient electric field was necessary. The problem was solved through igniting the microplasma by supplying a periodic voltage on the driving electrode. The interval of the power cycle was short enough to prevent repositioning of the bubble, but the repeated signal provided sufficient energy to ignite the plasma. Before microplasma ignition, the electrodes surrounding the bubble were supplied with high voltage to hold the bubble in place. Once the microplasma was ignited, the surrounding electrodes were turned off to avoid microplasma splitting shown in Fig. S1. ESI.‡ The periodic AC signal could then be continuously supplied to sustain the microplasma. It is important to note that the bubble in the plasma state was positioned by the high electric field opposite to the driving scheme of the original gas state. We attribute this phenomenon to the dramatic permittivity change of the bubble from the gas state to the plasma state. Plasma can be regarded as a conductive fluid full of ions and electrons.

After developing a method to ignite and position the microplasma in a bubble, we switched a high electric field along the driving electrodes to transport the microplasma. As shown in Fig. 5(a) and 5(b), the microplasma was ignited by periodically applying 655 V_{RMS}, 2.4 kHz on one of the driving electrodes. After the microplasma was ignited, the 655 V_{RMS}, 2.4 kHz was continuously applied (Fig. 5(b)). By turning on the adjacent

driving electrode and turning off the original one, the microplasma was moved to the left by one electrode each time as shown in Fig. 5(c) and 5(d). Video 2, ESI‡ shows footage of Fig. 5. Additionally, the captured images and video of transporting the microplasma in a dark environment can be found in Fig. S2 and Video 3 of the ESI‡.

Splitting the microplasma was demonstrated and is shown in Fig. 6. After igniting the microplasma using 587 V_{RMS}, 2.4 kHz (Fig. 6(a)), the microplasma was split from one bubble into two bubbles, as shown in Fig. 6(b) and 6(c). The microplasma on the right was extinguished, as shown in Fig. 6(d), because the driving electrode beneath it was turned off (Video 3, ESI‡).

Optical emission spectroscopy

The optical emission spectra of different bubbles were recorded by the optical spectrometer. A 200 nL air bubble was generated and ignited on the chip using the procedures described above. Fig. 7(a) shows the optical emission spectrum of the air microplasma. The characteristic peaks at the left side of Fig. 7(a) were primarily due to the emission from the N_2 second positive ($C^3\Pi_u$–$B^3\Pi_g$: 357.7, 375.5, and 380.5 nm) and the N_2^+ first negative ($B^2\Sigma_u^+$–$X^2\Sigma_g^+$: 391.4 nm) systems,[26] as magnified and shown in Fig. 7(b). Peaks at the right side of Fig. 7(a) can be assigned to the N_2 first positive system ($B^3\Pi_g$–$A^3\Sigma_u^+$).

The optical emission spectra of pure Ar and He gasses were also obtained from the microplasma in bubbles. The spectrum of Ar is shown in Fig. 8(a) with its characteristic peaks highlighted at the wavelengths of 484.8, 696.5, 706.7, 750.4, 811.5, and 842.4 nm.[26] We observed a major peak at 750.4 nm and other weaker, but observable, characteristic peaks. The spectrum of He is shown in Fig. 8(b) with its characteristic peaks highlighted at 492.1, 501.5, 587.5, 667.8, 706.5, and 728.1 nm.[24] With the ability to generate and mix bubbles and ignite the microplasma, the optical emission spectrum of the mixed Ar/He bubble was recorded and is shown in Fig. 8(c). The characteristic peaks of both Ar and He were found in the spectrum.

Conclusion

A microplasma emanating optical emission in a 200 nL bubble was demonstrated. The essential functions for preparing gas bubble samples of generating, merging, splitting, and expelling of bubbles in an inert silicone oil environment by DEP are reported. After the microplasma ignition, the microplasma was further manipulated by DEP. By analysing the spectra of the bubbles in the discharge state, air, two test gasses (Ar and He), and their mixture bubble could be identified using this approach. The ability to manipulate bubbles and the microplasma presents the potential for quantitative measurements of gas compositions and concentrations through sequential dilutions of the sample and reference bubbles with tunable ratios.

In the future, one of the gas reservoirs will be filled with an unknown gas sample. After mixing with the reference gas (*e.g.*, Ar or He) at a proper ratio in a bubble, the characteristic peaks of the microplasma radiation will be investigated for gas detection and analysis. However, we found that the microplasma would attack the dielectric layer and silicone oil. Hence, bubble expansion was observed, which will be detailed elsewhere and solved in future studies.

Acknowledgements

This work is supported by the National Science Council, Taiwan, R.O.C. under grants NSC 98-2221-E-009-129-MY3 and NSC 100-2120-M-009-004.

References

1 G. Kirchhoff and R. Bunsen, *The London, Edinburgh and Dublin Philosophical Magazine and Journal of Science*, 1861, **4**, 329–349.
2 M. A. Lieberman and A. J. Lichtenberg, *Principles of Plasma Discharges and Materials Processing, John Wiley, New York*, 1994.
3 J. C. T. Eijkel, H. Stoeri and A. Manz, *Anal. Chem.*, 1999, **71**, 2600–2606.
4 B. Mitra and B. Levey, *IEEE Trans. Plasma Sci.*, 2008, **36**, 1913–1924.
5 K. H. Becker and K. H. Schoenbach, *J. Phys. D: Appl. Phys.*, 2006, **39**, R55–R70.
6 F. Iza, G. J. Kim, S. M. Lee, J. K. Lee, J. L. Walsh, Y. T. Zhang and M. G. Kong, *Plasma Processes Polym.*, 2008, **5**, 322–344.
7 M. Laroussi and X. Lu, *Appl. Phys. Lett.*, 2005, **87**, 113902.
8 E. El Ahmar, C. Met, O. Aubry, A. Khacef and J. M. Cormier, *Chem. Eng. J.*, 2006, **116**, 13–18.
9 J. C. T. Eijkel, H. Stoeri and A. Manz, *Anal. Chem.*, 2000, **72**, 2547–2552.
10 J. K. Evju, P. B. Howell, L. E. Locascio and M. J. Tarlov, *Appl. Phys. Lett.*, 2004, **84**, 1668–1670.
11 D. R. Reyes, M. M. Ghanem and G. M. Whitesides, *Lab Chip*, 2002, **2**, 113–116.
12 J. Lim and D. R. Reyes, *Lab Chip*, 2003, **3**, 137–140.
13 M. Abdelgawad and A. R. Wheeler, *Adv. Mater.*, 2009, **21**, 920–925.
14 R. B. Fair, *Microfluid. Nanofluid.*, 2007, **3**, 245–281.
15 Y. Zhao and S. K. Cho, *Lab Chip*, 2007, **7**, 273–280.
16 S.-K. Fan and D.-Y. Lin, *Int. J. Autom. Smart Technol.*, 2012, **2**, 69–74.
17 H. Pellat, *C. R. : Acad. Sci. Paris*, 1895, **119**, 691–694.
18 J. R. Melcher and M. Hurwitz, *J. Spacecr. Rockets*, 1967, **4**, 864–871.
19 J. R. Melcher, D. S. Guttman and M. Hurwitz, *J. Spacecr. Rockets*, 1969, **6**, 25–32.
20 T. B. Jones, *J. Electrost.*, 2001, **51–52**, 290–299.
21 R. Ahmed and T. B. Jones, *J. Micromech. Microeng.*, 2007, **17**, 1052–1058.
22 S.-K. Fan, W.-J. Chen, T.-H. Lin and T.-T. Wang, *Lab Chip*, 2009, **9**, 1590–1595.
23 S.-K. Fan and T.-H. Hsieh, *Lab Chip*, 2009, **9**, 1236–1242.
24 S.-K. Fan, Y.-W. Hsu and C.-H. Chen, *Lab Chip*, 2011, **11**, 2500–2508.
25 U. Kogelschatz, *Plasma Chem. Plasma Process.*, 2003, **23**, 1–46.
26 R. W. B. Pearse and A. G. Gaydon, *The identification of molecular spectra*, Fourth Edition, John Wiley & Sons, Inc., New York, 1976.